13th World Conference on Earthquake Engineering
Vancouver, B.C., Canada
August 1-6, 2004
Paper No. 3375

THE HORIZONTAL DEFORMATION CHARACTERISTICS OF NATURAL RUBBER BEARING BY FEM ANALYSIS

Tomoki FURUTA[1]
Shinsuke ARAKI[2]

SUMMARY

In this study, the influence of flange rotation to horizontal deformation characteristics of laminating rubber bearing is investigated through FEM analysis. Analysis variables are shape of rubber bearings and rotation angle of upper flange. Analysis results present that horizontal stiffness decreases until shear strain (γ) of 200% in case of bearings with rotation. This tendency becomes larger as rotation angle becomes bigger. The decrement of horizontal stiffness in rotation angle (R) of 1/50 is remarkable. However, the influence of rotation can not be observed after shear strain of 200%. It is concluded that the structural design in mid-story isolation system is possible by estimate rotation angle of rubber bearings of R<1/150 and 10% reduction of horizontal stiffness.

INTRODUCTION

After the South Hyogo earthquake, seismic isolated buildings have been increasing rapidly. Recently, important buildings in earthquake disaster such as hospitals, the city hall and school are often constructed as isolated buildings. Furthermore, in a case of seismic upgrading for existing buildings, retrofit-isolation method has been major system.

Regardless of new constructions or retrofittings, there is a case to adopt mid-story isolation system by the reason such as shortening time, cost reduction, having many basement floors, limited space, and so on. In case of mid-story isolation system, isolation devices are installed in the top or central part of columns. However, the influence of deformations of columns to characteristics of isolation devices does not become clear.

In this study, the influence of rotation to horizontal deformation characteristics of laminating rubber bearing is investigated through FEM analysis, as shown in Fig. 1. In other words, the influence of bearing rotation to horizontal stiffness is estimated quantitatively.

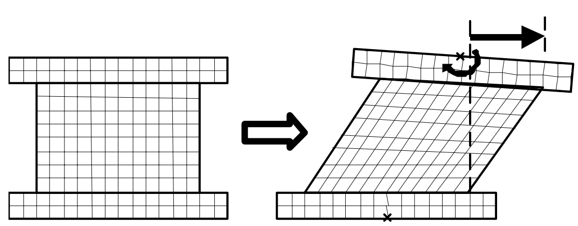

Fig. 1 Rotation of rubber bearing

[1] Damping & Isolation Unit, Technical Division, BANDO Chemical Industries, Ltd., Dr. Eng.
[2] Central Research Lab., BANDO Chemical Industries, Ltd., M. Eng.

METHOD OF ANALYSIS

Elements

As for the model shape, a 3-D model is adopted. The half of section of a radius direction is intended as shown in Fig. 2. A radius direction is divided in ten elements with 15 degrees as a standard using 3-D continuous solid elements (with 30 degrees for 45 degree-direction), a circular direction is divided into 4 elements with 1 cm around a center hole, the center, circumference, and a height direction is divided into two elements for one rubber layer and one intermediate steel plate each, and top and bottom flange is divided into four elements. The elements in which the strain distributions are investigated in detail are set smaller

These elements are decided taking the shape and numbers of the elements and calculation time into account (number of nods : 31231, number of elements : 26560, calculation time : 9h). A figure of whole model is shown in Fig. 3.

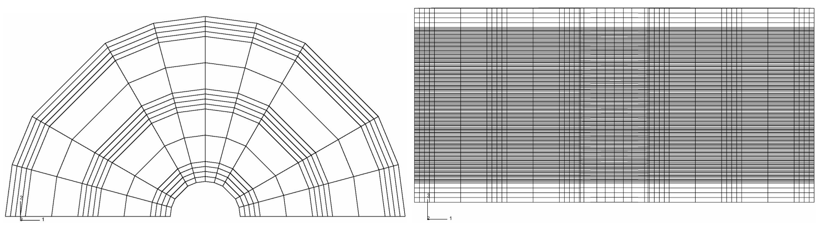

Fig. 2 Elements

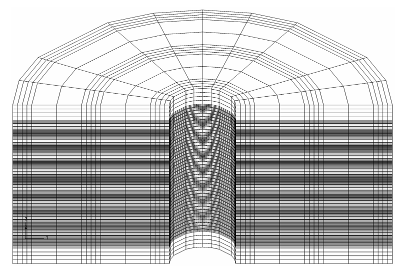

Fig. 3 Whole model

Rubber Materials

Rubber is modeled using the strain energy density function (W). In this analysis, the three dimensional polynomial expression shown in Eq.(1) is adopted taking into account the compression characteristic. [1] Mechanical elastic volume ratio and material constants of C_{ij}, D_{ij} are shown in Table 1. In addition, these constants shown in Table 1 are for nature rubber of shear elastic modulus (G) =0.4 N/mm^2.

$$W = \sum_{i+j=1}^{3} C_{ij}\left(\bar{I}_1 - 3\right)^i \left(\bar{I}_2 - 3\right)^j + \frac{1}{D_1}\left(J_{el} - 1\right)^{2i} \tag{1}$$

Where,

$\bar{I}_1$: primary permanence of declination strain $= \bar{\lambda}_1^2 + \bar{\lambda}_2^2 + \bar{\lambda}_3^2$

$\bar{I}_2$: secondary permanence of declination strain $= \bar{\lambda}_1^{(-2)} + \bar{\lambda}_2^{(-2)} + \bar{\lambda}_3^{(-2)}$

$\bar{\lambda}_i$: permanence elongation ratio $= J^{-1/3}\lambda_i$

J : volume ratio

J_{el} : mechanical elastic volume ratio

Table 1 Constants for rubber material

C_{10}	C_{01}	C_{20}	C_{11}	C_{02}
3.67×10^{-2}	-1.92×10^{-2}	6.55×10^{-4}	-1.09×10^{-3}	7.96×10^{-4}
C_{30}	C_{21}	C_{12}	C_{03}	D_1
-2.08×10^{-7}	0	0	1.07×10^{-6}	5.70×10^{-3}

The tensile test using dumbbell type No.3 specimens and pure shear test using 220 ˜15mm rectangle with 1mm thickness specimens are carried out for the purpose of obtaining the material constants. The constants are based on the regression analysis by the least square method using stress - strain relationships obtained by these tests.

Steel Plate

The intermediate steel plate is supposed to be elastic - plastic material with elastic modulus (E) =210,000 N/mm^2, and Poisson's ratio (ν) =0.3. Fig. 4 shows the model of intermediate steel plate used in this analysis. In this model, perfectly yielding takes place at strain (ε) =2 %.

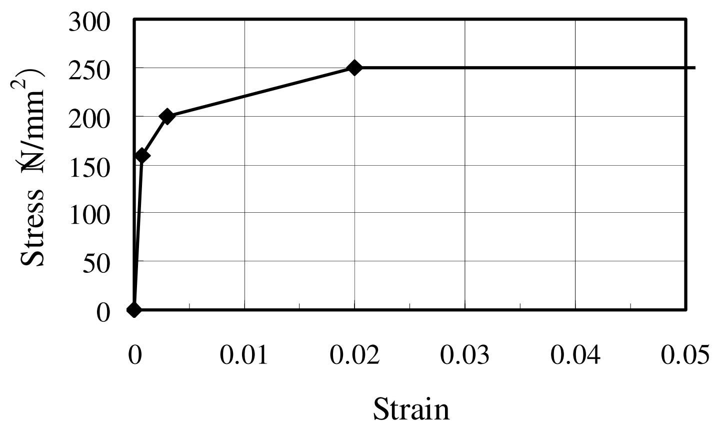

Fig. 4 Stress – strain model for steel plate

Boundary Conditions

As shown in Fig. 5, the virtual nodes (VN) are defined as it represents the degree of freedom of top and bottom surface of flanges. Vertical compressive force and horizontal shear force is applied to these two virtual nodes. The rotation is also applied only to top flange.

The rigid beams are set between the virtual nodes and nods of flange as shown in Fig. 6. Rotation of the virtual node makes whole flange rotation. In this analysis, y-coordinate of virtual node and flange node is set to same value as shown in Fig. 7. Rotation angle of the virtual node is exactly same with flange rotation. Because the half of section of a radius direction is intended in this analysis, deformation for z-axis and rotation for y-z plane is restricted in cutting section as shown in Fig. 8.

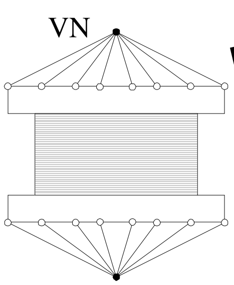

Fig. 5 Virtual Node

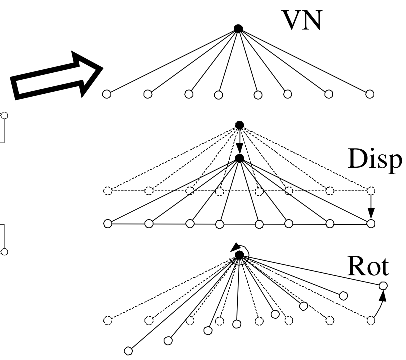

Fig. 6 VN action

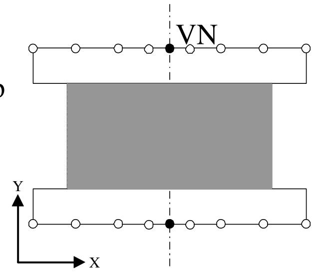

Fig. 7 Boundary condition

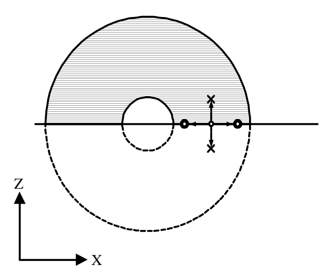

Fig. 8 Section condition

Analysis Step

The order of analysis is as follows (Fig. 9);

Step 1 : The rotation angle is applied to virtual nodes as a target value.

Step 2 : Vertical compression force is applied.

Step 3 : Horizontal displacement is applied with the interval of shear strain (γ) of 100% from 100% to 400%

Analysis is done till it becomes unstable, and results are output with free range. In this analysis, 3-D non-linear FEM Code ABAQUAS ver6.2 is used.

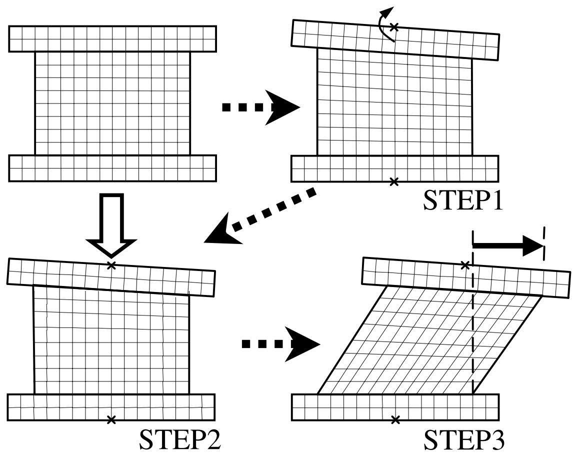

Fig. 9 Analysis step

ANALYSIS VARIABLES

Analyzed Bearing

Three types of bearing shown in Table 2 are analyzed. Rubber materials have same characteristics with shear elastic modulus (G) =0.4 N/mm^2. Outer diameter (D) =800mm, primary shape coefficient (S_1) =33.0, second shape coefficient (S_2) =4.00 for No.1 bearing, for No. 2 bearing, D =700mm, S_1=29.5, S_2=3.50, and D =700mm, S_1=35.4, S_2=4.96 for No.3 bearing. No.1 and No.2 bearing is LRB type with total rubber thickness of 200mm, and No.3 bearing have S_2=5 type specification. However, the analysis is carried out only for rubber and steel plates in No.1 and No.2 bearings.

Table 2 Shape of analyzed bearing

No.	Outer diameter (mm)	Inner diameter (mm)	Rubber thickness (mm)	Number of laminating	Total Rubber thickness (mm)	Steel Plate thickness (mm)	S_1	S_2
1	800	140	5.0	40	200.0	2.8	33.0	4.00
2	700	110	5.0	40	200.0	2.5	29.5	3.50
3	700	35	4.7	30	141.0	3.1	35.4	4.96

Analysis Variables

The standard analysis is set to the case of no rotation angle of flange. Only vertical compression force and horizontal shear displacement is applied (R=0). Vertical force (axial stress, σ) is set to σ=10N/mm^2 for all cases. The variable is rotation angle of flange as R=1/500 (0.115 degree), 1/200 (0.286 degree), 1/150 (0.382 degree), 1/100 (0.573 degree), 1/75 (0.764 degree), 1/50 (1.146 degree).

RESULTS OF ANALYSIS

Comparison between Analysis and Experimental Result

The comparison between analytical shear stress (τ) - shear strain (γ) relationships with experimental results for the bearing shown in Table 2 is conducted in order to confirm precision of this FEM analysis. Because it is very difficult to carry out experimental test for the bearing with rotation angle, the influence of bearing rotation to horizontal stiffness will be discussed only by using FEM results. In order to confirm the adaptability between analysis and experimental test, comparison between analytical results and experimental ones for the bearing without rotation is done.

Comparisons of τ - γ relationships of experiment and analysis are shown in Fig. 10 - Fig. 12. Solid lines and dotted lines show experimental and analytical data, respectively. Fig. 10 (No.1) and Fig. 11 (No.2) is for the bearings in which inner diameter (d_i) is relatively bigger comparing to outer diameter (D). Buckling failure takes place in this type of bearing with second shape coefficient (S_2) <4.0. The details about buckling refer to literature [2].

It is considered that analytical results have a good agreement with experimental results in general. In detail, experimental shear stress show bigger value rather than analytical one until around shear strain (γ) =150%, and after that analytical stress becomes bigger than experimental one. The reason of this is considered that modeling of rubber bearing under axial stress (modeling based on the shear test for the materials taking axial stress variables into account) have some problems. As for this, the ratio of vertical compression force (axial stress σ=10N/mm2) to buckling stress (σ_{cr})[3] (No.1 : 51.7N/mm^2, No.2 : 47.8N/mm^2 ）show a value of $\sigma/\ \sigma_{cr}$ =0.2 at γ=0%. Because this value is higher than standard axial stress which is used for design (σ_0 : specification stress for dead load, No.1 : 9.0N/mm^2, No.2 : 6.5N/mm^2), it does not become clear for reproduction of

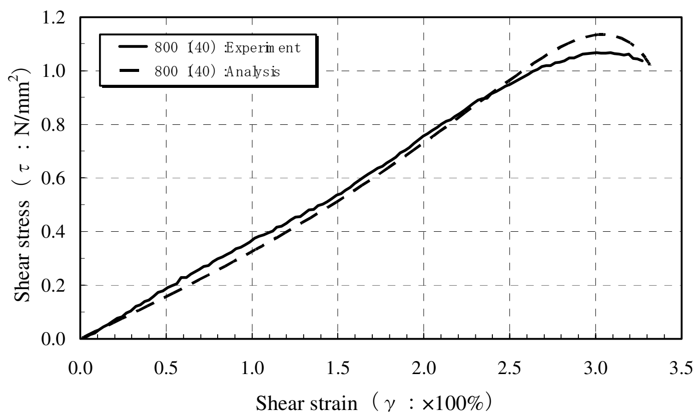

Fig. 10 No.1(D=800, d_i=140, S_1=33.0, S_2=4.00)

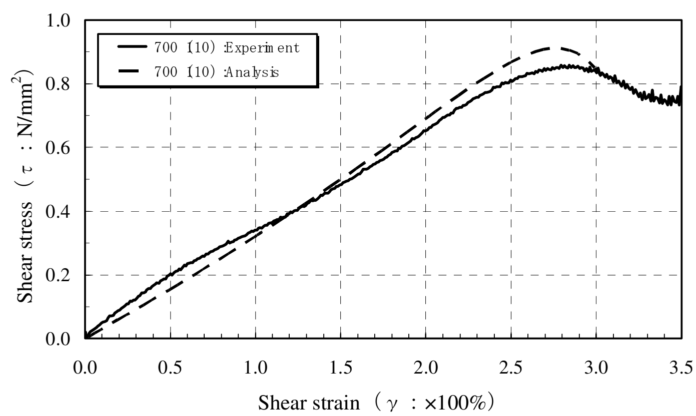

Fig. 11 No.2(D=700, d_i=110, S_1=29.5, S_2=3.50)

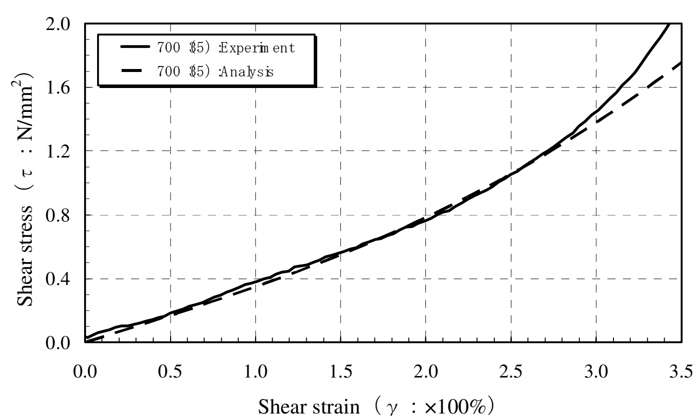

Fig. 12 No.3(D=700, d_i=35, S_1=35.4, S_2=4.96)

dependency.

The rubber strain shows hardening region level, however, under high stress in local by bearing rotation. Therefore, it is supposed that modeling of rubber material used in this analysis have little problem. In addition, strain at which buckling takes place (stress reduction) is well represented by analysis. It is considered that modeling of intermediate steel plate is reliable, because it is important factor to represent buckling.

Fig. 12 (No.3) is for the bearings in which inner diameter (d_i) is relatively smaller comparing to outer diameter (D). Buckling failure hardly takes place in this type of bearing with second shape coefficient (S_2) =5.0. From Fig. 12, the analysis can represent the experimental result well until γ =300%. The difference between analysis and experiment after γ =300% is caused by scattering of rubber characteristics in hardening region. In addition, σ_{cr} =60.1N/mm^2 and σ / σ_{cr} =0.16 (σ=10 N/mm^2) in No.3, axial stress is smaller than specified value (σ_0 =13N/mm^2). Therefore, in a low axial stress less than σ_0, modeling with axial stress considering is not necessary.

From these comparisons between analysis and experiment, it can be concluded that this FEM analysis can perform τ - γ relationships very well in case of no rotation (R=0) of flange.

Analysis with Flange Rotation

Deformations around the edges and inner hole at rotation angle (R) of 1/50 are shown in Fig. 13 - Fig. 15. Fig. 13 and Fig. 14 shows the part of compression and tension region, respectively. Though triangle deformation is observed because of two-divided elements, actual deformation is assumed as shown in Fig. 16. Rubber is expanded in compression region and becomes hollow in tensile region. These deformation characteristics are easily supposed in non-compression materials with a little free surface between inner steel plates. It is considered that these deformations correspond with actual deformations. It is difficult to

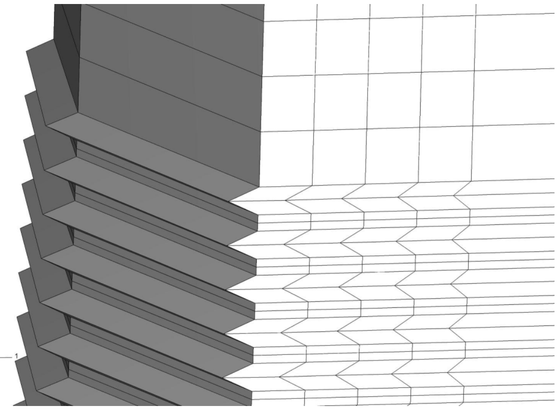

Fig. 13 Compression part

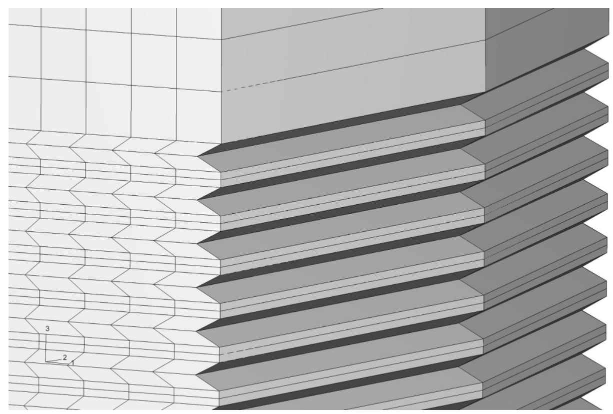

Fig. 14 Tension part

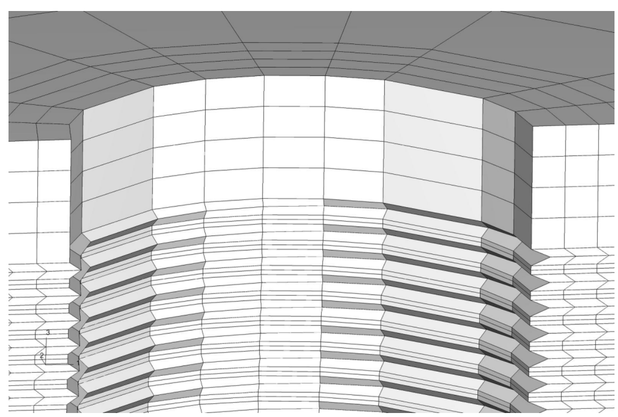

Fig. 15 Inner hole

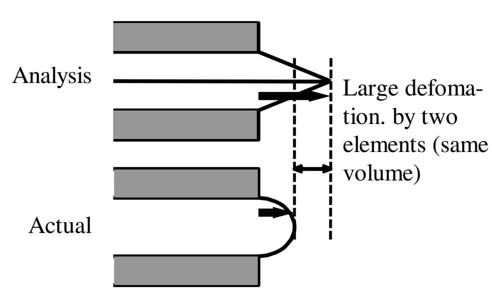

Fig. 16 Actual deformation

observe the state of deformation in actual bearings because of cover rubber. In addition, large shear stress may act on adhesive interface between rubber and steel plate due to quantity of rubber deformation.

Shear stress (τ) - shear strain (γ) curves of analyzed bearings shown in Table 2 with flange rotation angles (R=0, 1/500, 1/200, 1/150, 1/100, 1/75, 1/50) are shown in Fig. 17 - Fig. 19. Because calculation could not be completed for No.3 in Fig. 19 due to large deformation caused by rotation, τ - γ curves is interrupted around γ =200%.

In all cases, shear stress and horizontal stiffness becomes smaller as rotation angle becomes larger until around γ=200%. The decrement of horizontal stiffness in R=1/50 is remarkable. On the other hand, τ - γ curves after γ=200% are almost similar regardless of rotation angle. The remarkable influence of horizontal stiffness by rotation angle can not be recognized after γ =200%. The strains at which hardening and buckling occurs are almost same in all rotation cases.

Fig. 21 - Fig. 23 show horizontal stiffness ratio of each rotation angle divided by stiffness of rotation angle R=0 in order to compare quantitatively. In these figures, horizontal stiffness is defined as secant modulus (Q / δ) in each shear strain as shown in Fig. 20.

Horizontal stiffness becomes lower in case of small shear strain (γ). This tendency is recognized remarkably as rotation angle is bigger. However, little changing of horizontal stiffness is observed after γ=200% regardless of rotation level.

Scattering of horizontal stiffness in production of actual bearing is specified as ±10~15% in the term of dependency of axial pressure and shear strain level. It can be said that changing range of ±10% is permitted in actual design. The rotation angle at which changing ratio of horizontal stiffness is smaller than ±10% is R <1/150. Therefore, the structural design in mid-story

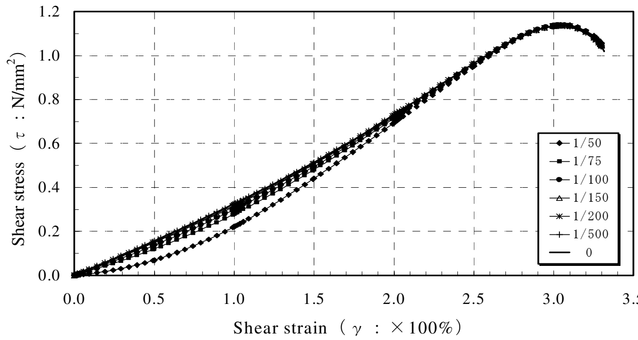

Fig. 17 No.1(D=800, d_i=140, S_1=33.0, S_2=4.00)

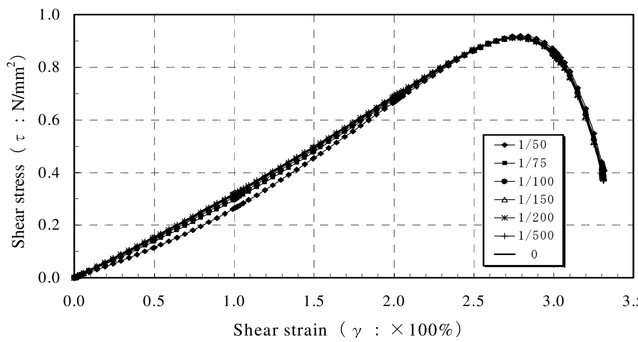

Fig. 18 No.2(D=700, d_i=110, S_1=29.5, S_2=3.50)

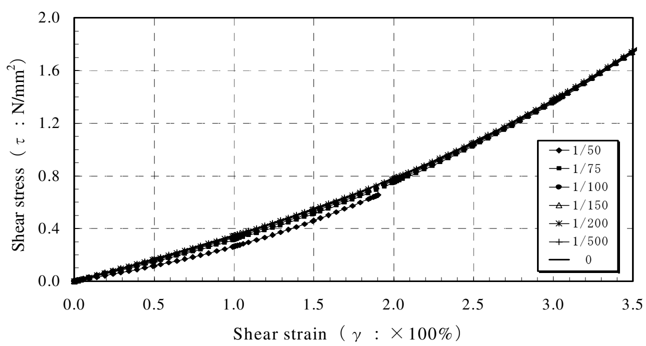

Fig. 19 No.3(D=700, d_i=35, S_1=35.4, S_2=4.96)

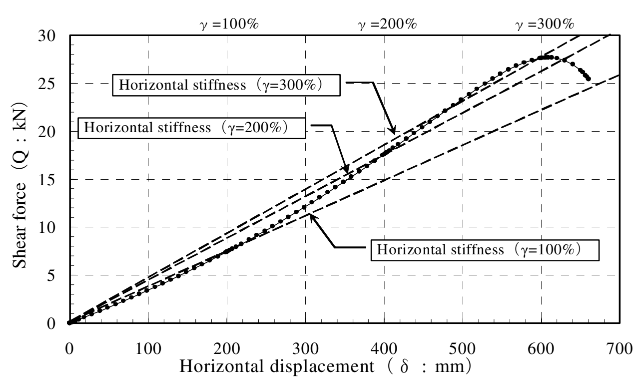

Fig. 20 Definition of horizontal stiffness

isolation system (top-column isolation) is possible by estimate following two items.
(1) The rotation angle of rubber bearings is smaller than 1/150 (0.4 degree).
(2) The reduction of horizontal stiffness of 10% is considered.

However, more investigations are necessary for other bearings which are not simulated in this analysis. Furthermore, the experimental test has not been done yet because of difficulty of loading. From the results of this analysis, it is considered that the influence of rotation in the range of ordinary structural design level (γ < 200 - 250%) can be predicted due to analysis precision as shown in Fig. 10 - Fig. 12.

CONCLUSIONS

As a result of FEM analysis which is conducted to investigate the influence of rotation of rubber bearing, the followings are concluded.

1. This analysis results is reliable in representing shear stress (τ) - shear strain (γ) relationships by comparing with experimental results in case of no-rotation angle.
2. Analysis results show that horizontal stiffness decreases until γ=200% in case of bearings with rotation.
3. This tendency becomes larger as rotation angle becomes bigger. The decrement of horizontal stiffness in R=1/50 is remarkable.
4. The influence of rotation can not be observed after γ=200%.
5. The strains at which hardening and buckling occurs are almost same in all rotation cases.
6. The rotation angle at which changing ratio of horizontal stiffness is smaller than ±10% is R < 1/150.
7. The structural design in mid-story isolation system is possible by estimate rotation angle of rubber bearings of R<1/150 and 10% reduction of horizontal stiffness.

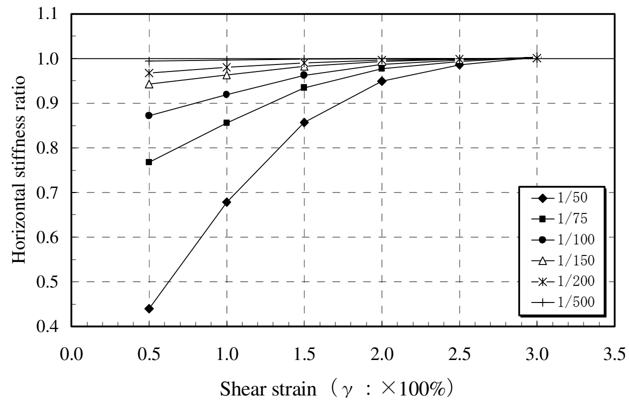

Fig. 21 No.1(D=800, d_i=140, S_1=33.0, S_2=4.00)

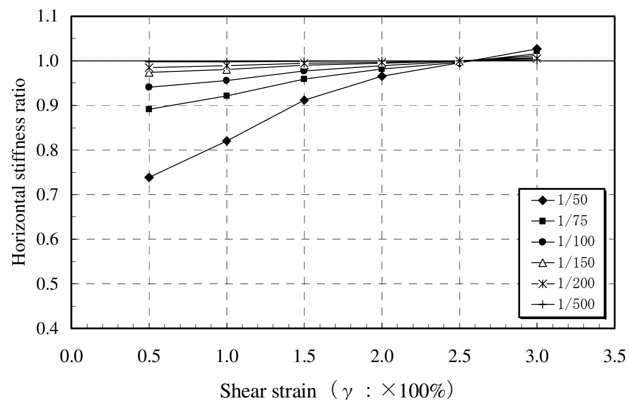

Fig. 22 No.2(D=700, d_i=110, S_1=29.5, S_2=3.50)

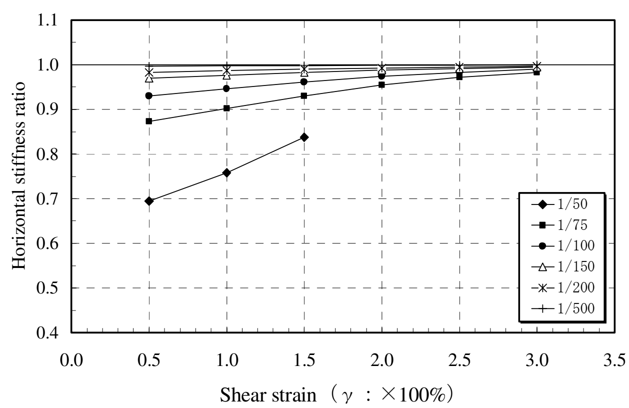

Fig. 23 No.3(D=700, d_i=35, S_1=35.4, S_2=4.96)

In this analysis, variation of bearing shapes and axial stress is limited because of consideration of the comparison between analysis and experiment. At the present, it becomes possible to obtain inner steel plate strain by strain gauge measurements until ultimate stage. In addition, the experimental test to apply rotation is very dangerous, and considerable devices are necessary for loading jigs. The jig which can coordinate a rotation angle with level of horizontal deformation is being produced currently.

REFERENCES

[1] The society of rubber industry Japan, "The handbook of the rubber-metal laminated bearing for seismically isolated structure", 2000, pp.45-46.

[2] Furuta, T., Araki, S. and Matsuoka, H., "Characteristics of Interlayer Steel Plate in Rubber Bearing at Buckling", Summaries of technical papers of annual meeting Architectural Institute of Japan, Structure 2, 2001, pp.637-640

[3] Architectural Institute of Japan, "Recommendation for the Design of Base Isolated Buildings", 2001, pp.33-34.